

# Mechanism by which nodakenin inhibits the AURKA-CXCL5 axis to intervene in the phenotype of non-small cell lung cancer

X. Wang<sup>1#</sup>, R. Tian<sup>2#</sup>, K. Duan<sup>3</sup>, X. Zhang<sup>4\*</sup>

<sup>1</sup>Department of Western Medicine Pharmacy, Baoding No. 1 Central Hospital, Baoding, China

<sup>2</sup>Department of Oncology, Hospital of the People's Liberation Army, 82<sup>nd</sup> Group Army, Baoding, China

<sup>3</sup>General Surgery, Sanhe City Hospital in Hebei Province, Sanhe, China

<sup>4</sup>Department of Ultrasound, Affiliated Hospital of Hebei University, Baoding, China

## ABSTRACT

### ► Original article

#### \*Corresponding author:

Xu Zhang, M.D.,

E-mail: xuzhang0312@163.com

Received: March 2025

Final revised: July 2025

Accepted: July 2025

Int. J. Radiat. Res., January 2026;  
24(1): 69-74

DOI: 10.61186/ijrr.24.1.11

**Keywords:** Nodakenin, AURKA-CXCL5, NSCLC, DNA damage repair, neoplastic cell phenotype, aurora kinase A.

**Background:** This study investigates the mechanism by which the natural flavonoid drug Nodakenin intervenes in the phenotype of non-small cell lung cancer (NSCLC) by inhibiting the aurora kinase A-C-X-C motif chemokine ligand 5 (AURKA-CXCL5) axis, and analyses its role in enhancing tumour sensitivity to radiotherapy. **Materials and Methods:** Human NSCLC A549 cells were classified into control group (CG), radiation group (RG), and Nodakenin group (NG). Radiotherapy was delivered at 2 Gy/day for five days using 6 MV X-rays. Nodakenin (10 µM) was applied for 24 h after irradiation. Cell proliferation and survival were assessed using the MTT assay and the colony formation assay. Apoptosis was assessed by Annexin V-FITC/PI staining and flow cytometry. Gene expression of AURKA and CXCL5 was quantified by quantitative polymerase chain reaction (qPCR), DNA damage by γ-H2AX immunofluorescence, and apoptotic proteins by Western blotting. **Results:** The AURKA/CXCL5 mRNA in the RG surpassed that observed in the CG (P<0.05), while the AURKA/CXCL5 mRNA in the NG was lower than RG (P<0.05). The γ-H2AX in the NG exceeded that in the RG. The cell viability in the NG was below that in the RG (P<0.05), and the apoptosis rate in the NG exceeded that in the RG (P<0.05). The quantity of cell migration and invasion in the NG was lower than RG (P<0.05). The Bax and caspase-3 proteins in the NG exceeded that in the RG (P<0.05), while the Bcl-2 was lower (P<0.05). **Conclusion:** Nodakenin exacerbates DNA damage and apoptosis by inhibiting the AURKA-CXCL5 axis, thereby suppressing tumor cell proliferation and invasion.

## INTRODUCTION

Globally, NSCLC comprises about 85% of lung cancer cases. Surgical operation is an effective system for lung cancer treatment. Anatomic lobectomy is the preferred surgical method, which can effectively remove the tumor lesions, with small trauma and fast recovery. Radiotherapy is an approach to treat NSCLC, but its effect is limited by the sensitivity of tumor to radiation. Therefore, improving the sensitivity of tumor to radiotherapy is one of the key strategies to optimize the prognosis. Nodakenin is a natural flavonoid obtained from Chinese herbal medicines such as Scutellarin baicalensis Georgi and Peucedanum. It has been widely used due to its extensive pharmacological activities, containing anti-inflammatory, anti-oxidation, and anti-tumor properties (1, 2). In the research of NSCLC, two molecular markers, AURKA and CXCL5, have attracted attention. AURKA is an essential kinase involved in regulating the cell cycle, often over-expressed in tumors and associated with tumor cell proliferation, migration, and resistance to chemotherapy and radiotherapy (3). CXCL5 is a chemokine that exerts a

significant effect in controlling the inflammatory response within the tumor micro-environment and accelerate the invasion and spread of tumor cells (4,5). The AURKA-CXCL5 signaling axis is crucial in modulating tumor cell treatment responses. Yang et al. investigated the AURKA in immune escape in lung adenocarcinoma, revealing that the ETS variant transcription factor 4 (ETV4)/AURKA axis mediates the immune escape mechanism in lung adenocarcinoma by adjusting the Janus kinase 2/signal transducer and activator of transcription 3 (JAK2/STAT3) (6). Lei et al. constructed an in vitro model of macrophages co-cultured with NSCLC cells, revealing that adenosine activates nuclear factor kappa-light-chain-enhancer of activated B cells (NFκB) through adenosine A2A receptor (A2AR), thus up-regulating CXCL5 expression in macrophages (7). Du et al. proposed AURKA for cancer treatment (8). Park et al. studied the interaction mechanism between CEP192 and AURKA, revealing the regulatory mechanism of AURKA activity and subcellular localization during mitosis (9). Wang et al. sought to clarify the prognostic assessment and treatment targets for lung adenocarcinoma. Through

comprehensive bioinformatics analysis and in vitro experiments, they found that AURK was highly expressed in lung cancer tissues and was associated with advanced tumors and poor prognosis<sup>(10)</sup>.

Nodakenin, as a natural mixture, can inhibit the expression of inflammatory factors. Shah et al. found that Nodakenin exerts a colon-protective effect through the NF- $\kappa$ B-mediated NLRP3 inflammasome pathway and can downregulate the expression of TNF- $\alpha$ , IL-6, NF- $\kappa$ B, etc.<sup>(11)</sup>. The results of Chung *et al.*'s study revealed the efficacy of Nodakenin in colorectal cancer. Nodakenin can inhibit tumor progression in a colon cancer mouse model induced by a HFD/AOM/DSS<sup>(12)</sup>. Nodakenin changed the biological behavior of NSCLC cells, especially its sensitivity to radiotherapy, by interfering with the AURKA-CXCL5 axis<sup>(13)</sup>. Preliminary studies indicate that nodakenin suppresses AURKA and CXCL5 expression, thereby hindering tumor cell proliferation and survival, increasing sensitivity to radiation-induced DNA damage, and promoting apoptosis<sup>(14)</sup>. This study investigates how nodakenin inhibits the AURKA-CXCL5 axis to alter NSCLC phenotypes and enhance radiosensitivity. The research aims to elucidate nodakenin's role in modulating NSCLC cell phenotypes via the AURKA-CXCL5 axis and improving tumor cell radiosensitivity, providing a scientific foundation for new NSCLC treatment strategies. The novelty of the study lies in revealing that the natural compound Nodakenin optimizes the radiosensitivity of NSCLC by inhibiting the signaling axis constituted by AURKA and CXCL5.

## MATERIALS AND METHODS

### Cell models and growth conditions

The NSCLC A549 cells were from the DSMZ (German Collection of Microorganisms and Cell Cultures) (Cat# ACC 310, Braunschweig, Germany). Through short tandem repeat (STR) analysis and identification, no mycoplasma contamination was found. Following storage in liquid nitrogen, the cells were rapidly thawed in a humidified incubator maintained at 37 ° C with 5% CO<sub>2</sub> for 30 minutes. The cells were maintained in RPMI-1640 (Sigma-Aldrich, Cat# R8758, USA) enriched with 10% fetal bovine serum (FBS) (Cellmax, Cat# C0502, China) and 1% penicillin-streptomycin solution (Solarbio, Cat# P1400, China). To ensure that the cells are in a good growth environment, the frequency of medium replacement is set to once every 2-3 days. In this case, 80-90% of the fused cells will undergo division in a ratio of 1:3.

### Medications and treatment

Nodakenin is a coumarin compound with a purity of  $\geq 98\%$ , obtained from Shanghai Yuanye Biotechnology Co., Ltd. (Cat# B21279). In the

intervention group, Nodakenin at 10  $\mu$ M was added after radiotherapy treatment, and incubation was continued for 24 h.

### Grouping and processing

A549 cells were separated into CG, RG, NG. Cells in the RG group were irradiated with 6 MV X-rays using a linear accelerator for 5 days at 2 Gy/day. Cells in the NG group were subjected to 10  $\mu$ M Nodakenin after radiation and incubated for 24 h. Cells in the CG group did not receive radiation therapy.

### Real-time fluorescent qPCR

Extract total RNA was extracted from cells using RNAiso Plus reagent (Takara, Japan; Cat# 9109), and reverse transcription was performed using a gDNA-removal cDNA synthesis kit (Thermo Fisher Scientific, Cat# K1622, USA). Perform qPCR reactions using AceQ SYBR Green qPCR Master Mix (Vazyme; Cat# Q111) on the QuantStudio 5 system (Applied Biosystems, USA). Calculate relative expression levels using the 2<sup>- $\Delta\Delta$ Ct</sup>, with GAPDH (Proteintech, China; Cat# 60004-1-Ig) as the internal control.

### Immunofluorescence staining detection of $\gamma$ -H2AX

Seed cells were onto 24-well plates. After irradiation with 4 Gy, fix cells with 4% paraformaldehyde for 0.33h, penetrate with 0.2% Triton X-100 for 0.33h, and block with 5% bovine serum albumin for 0.5h. Incubate the cells with  $\gamma$ -H2AX antibody (Abcam, UK; Cat# ab26350) overnight, followed by FITC-conjugated goat anti-mouse IgG secondary antibody (Thermo Fisher Scientific, USA; Cat# A16073) and DAPI (Servicebio; Cat# G1012) for nuclear staining. Acquire images using a laser confocal microscope (A1R, Nikon, Japan).

### Cell proliferation assay

Seed cells at  $1 \times 10^4$  cells per well in a 96-well plate. On days 1, 3, and 5, add 20  $\mu$ L of 5 mg/mL MTT solution (Beyotime, Cat# ST316) to each one, incubate for 4h, then remove the clear upper layer. Add 150  $\mu$ L of DMSO (Sigma-Aldrich, USA; Cat# D8418) to dissolve the MTT crystals, oscillate for 0.17h, and read the optical density at 490 nm to evaluate cell viability. In the colony formation assay, culture cells for 14 days post-irradiation, and count the number of colonies after crystal violet staining to evaluate radiation resistance.

### Flow cytometry analysis of apoptosis

After irradiation with 8 Gy, incubate cells for 48h, digest with trypsin without ethylenediaminetetraacetic acid (EDTA), wash with phosphate-buffered saline (PBS), and stain with Annexin V-FITC/PI using a commercial apoptosis detection kit (Beyotime, Cat# C1062M). Samples were analyzed with a SH800S flow cytometer (Sony

Biotechnology, Japan).

### Cell motility and invasiveness assays

Cell motility and invasiveness assays were conducted using Transwell chambers (Corning, Cat# 3422). For the motility assay,  $5 \times 10^4$  cells were seeded into the upper compartment in serum-free medium, while the lower compartment contained medium supplemented with 10% FBS. For the motility assay, Matrigel (Cat# 356234) coating was applied to the upper chamber prior to the assay, and  $2 \times 10^5$  cells were added to each well. After 24 hours of incubation, cells were stained with crystal violet and subsequently quantified.

### Western blot analysis of protein expression

Extract total protein by radioimmunoprecipitation assay (RIPA) buffer (Thermo Fisher Scientific, USA; Cat# 89900). Measure protein concentrations with a bicinchoninic acid (BCA) assay kit (Beyotime, China; Cat# P0010). Performed SDS-PAGE with 4–20% Tris-Glycine gels (Thermo Fisher Scientific, USA; Cat# XP04205BOX). Transfer proteins to PVDF membranes (Millipore, USA; Cat# IPVH00010). Following blocking, membranes were exposed to primary antibodies and then with HRP-labeled secondary antibodies (Proteintech, Wuhan, China). Detect signals by enhanced chemiluminescence (ECL) reagents (Thermo Fisher Scientific, USA; Cat# 32106). Protein bands were imaged using the Tanon 5200 system (Tanon, China).

### Radiation conditions

All radiotherapy was performed using a 6 MV X-ray generated by an Elekta Synergy medical linear accelerator (Elekta AB, Sweden). The treatment group received 2 Gy (266 mu) daily for 5 consecutive days (total dose of 10 Gy). The irradiation dose for the immunofluorescence experiment was 4 Gy per session; the apoptosis experiment used 8 Gy per session, followed by 48 h of culture after irradiation.

### Statistical analysis

Display all data as average standard deviation (SD). SPSS 11.5 was taken for statistical significance analysis, and Bonferroni method was adopted for variance analysis. Statistical significance was defined as  $P < 0.05$ .

## RESULTS

### Nodakenin inhibits the expression of AURKA-CXCL5 axis

The results of qPCR assay for AURKA/CXCL5 expression are shown in table 1. The AURKA/CXCL5 mRNA in the RG exceeded that in the CG ( $P < 0.05$ ), while the AURKA/CXCL5 mRNA in NG was below that in the RG ( $P < 0.05$ ). Nodakenin inhibited the up-regulation of AURKA/CXCL5 axis expression

induced by radiation.

**Table 1.** mRNA expressions of AURKA and CXCL5 in A549 cells (qPCR detection). CG: control group; RG: radiation group (2 Gy/day, 5 days); NG: irradiation + Nodakenin group (10  $\mu$ M); AURKA: mitotic protein kinase A; CXCL5: CXC motif chemokine ligand 5.

Group	AURKA	CXCL5
CG	1.09 $\pm$ 0.04	1.04 $\pm$ 0.02
RG	1.96 $\pm$ 0.15	2.02 $\pm$ 0.20
NG	1.27 $\pm$ 0.11	1.18 $\pm$ 0.07
Variance ratio	10.307	12.614
P-value	0.016	0.027

### Inhibition of AURKA/CXCL5 axis can promote DNA damage induced by radiotherapy and enhance the radiosensitivity

Figure 1 and table 2 explain the immunofluorescence staining analysis of  $\gamma$ -H2AX. The  $\gamma$ -H2AX in CG was below that in the RG and the NG ( $P < 0.05$ ), while that in NG exceeded that in the RG. The red signal of  $\gamma$ -H2AX in the CG was less and the DNA damage was lower. The RG showed moderate red signals, indicating DNA damage and cellular response to radiation therapy. Compared with the RG, the NG had the strongest  $\gamma$ -H2AX red signal, high DNA damage, and increased cell sensitivity to radiation ( $P < 0.05$ ).

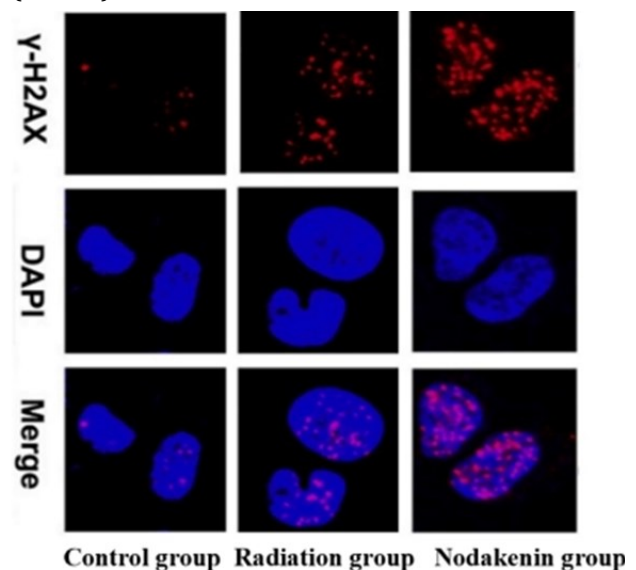


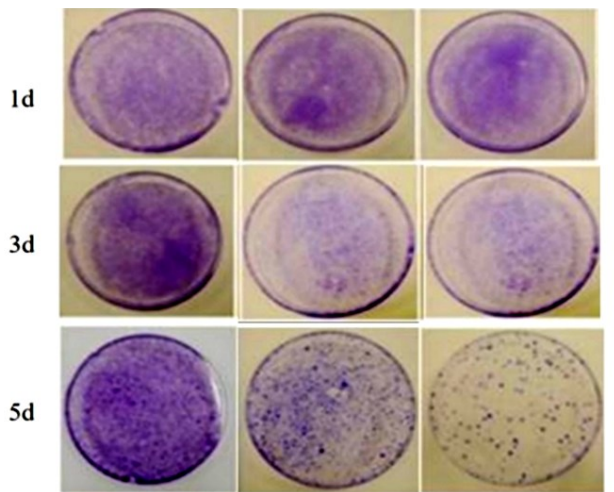
**Figure 1.** Immunofluorescence Staining. A549 cells were divided into CG, RG (2 Gy/day for 5 days), and NG (10  $\mu$ M Nodakenin added after irradiation). DNA double-strand breaks were labelled with  $\gamma$ -H2AX (red), and nuclei were stained with DAPI (blue). Compared with the CG,  $\gamma$ -H2AX expression was enhanced in the RG and even more significantly in the NG, suggesting that Nodakenin promotes radiotherapy-induced DNA damage and enhances radiosensitivity. Scale bar: 50  $\mu$ m.

**Table 2.** Immunofluorescence Quantification Results of  $\gamma$ -H2AX Expression Levels in A549 Cells. CG: control group; RG: radiation group; NG: irradiation + Nodakenin group.

Group	$\gamma$ -H2AX
CG	1.02 $\pm$ 0.02
RG	1.57 $\pm$ 0.13
NG	2.11 $\pm$ 0.18
Variance ratio	12.445
P-value	0.003

### Nodakenin increases the radiosensitivity of cells

The radiosensitivity analysis of Nodakenin-increased cells is shown in figure 2 and table 3. On the 1st day, the cell proliferation ability of the CG was stronger than that of the RG and NG ( $P<0.05$ ), but no obvious difference existed between RG and NG ( $P<0.05$ ). On the 3<sup>rd</sup> and 5<sup>th</sup> day, the cell proliferation ability of the NG was below that of the CG and the RG ( $P<0.05$ ), and nodakenin increased the sensitivity of cells to radiation. The colony-formation test demonstrated that compared with the CG, radiation could reduce the colony-formation ability of cells ( $P<0.05$ ), and nodakenin obviously added the toxic effect of radiation on cells ( $P<0.05$ ).



Control group Radiation group Nodakenin group

**Figure 2.** Cell colony-formation test. Cells in the CG, RG, and NG were treated before and after irradiation, and crystal violet staining was used to observe colony formation after 14 days of culture. The number of colonies decreased in the RG and further decreased in the NG, indicating that Nodakenin can enhance the inhibitory effect of radiotherapy on cell proliferation.

**Table 3.** Cell viability assay results for A549 cells at different time points. CG: control group; RG: radiation group; NG: radiation + Nodakenin group

Group	1d	3d	5d
CG	0.35±0.02	0.74±0.10	1.36±0.14
RG	0.27±0.01	0.44±0.05	0.75±0.08
NG	0.26±0.02	0.31±0.02	0.42±0.04
Variance ratio	11.773	9.516	13.451
P-value	0.019	0.008	0.003

### Detection of cell viability and apoptosis rate

The comparison of cell survival and apoptosis rates among different groups is presented in table 4. The cell viability of the CG exceeded that of the RG and the NG ( $P<0.05$ ). The cell viability of the CG was below that of the RG and the NG ( $P<0.05$ ), that of the NG was below the RG ( $P<0.05$ ), and that of the NG exceeded the RG ( $P<0.05$ ).

### Detection of cell motility and invasiveness

The cell motility and invasiveness assays are presented in figure 3 and table 5. The cell motility

and invasiveness in the CG exceeded that in the RG and the NG ( $P<0.05$ ), and the cell migration in the NG exceeded that in the RG ( $P<0.05$ ).

**Table 4.** Comparison of cell viability and apoptosis rates among different groups of A549 cells. CG: control group; RG: radiation group; NG: radiation + Nodakenin group.

Group	Cell viability	Apoptosis rate
CG	84.24±5.17	11.37±3.24
RG	55.32±4.88	34.66±4.11
NG	37.51±3.86	52.38±5.31
Variance ratio	15.303	9.664
P-value	0.002	0.013

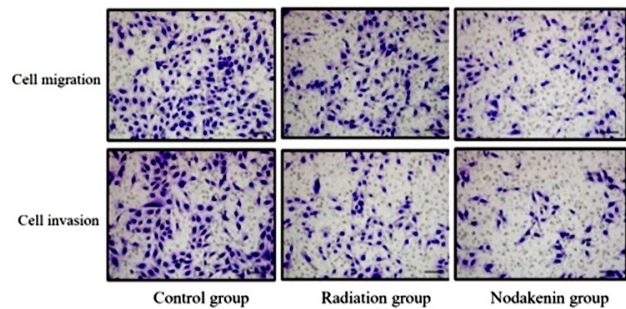


**Figure 3.** Cell motility and invasiveness test. Transwell chambers conduct migration and invasion experiments. The motility and invasiveness abilities of cells in the RG decreased compared to those in the CG, and further decreased in the NG, indicating that Nodakenin can synergistically inhibit the motility and invasiveness potential of tumor cells with radiotherapy.

**Table 5.** Transwell assay results for A549 cell motility and invasiveness capabilities. CG: control group; RG: radiation group; NG: radiation + Nodakenin group.

Group	Cell migration	Cell invasion
CG	155.28±16.49	137.68±13.22
RG	127.39±14.88	93.27±10.66
NG	94.65±10.27	63.49±8.05
Variance ratio	15.266	11.287
P-value	0.011	0.004

### Analysis of apoptosis protein expression

The apoptotic proteins and their blotting analysis results are presented in figure 4 and table 6. The *Bax*, *Bcl-2* and *caspase-3* in the RG exceeded that in the CG ( $P<0.05$ ), while the *Bcl-2* was below that in the CG ( $P<0.05$ ). The *Bax* and *caspase-3* protein increased in the NG raised ( $P<0.05$ ), while the *Bcl-2* declined ( $P<0.05$ ).

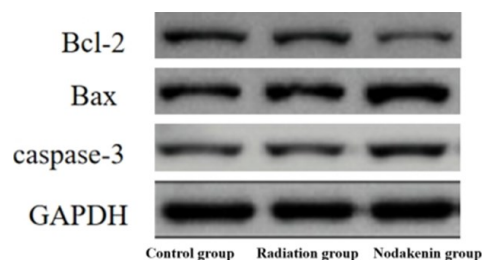


**Figure 4.** Analysis of apoptosis protein expression. Western blot analysis detects the *Bax*, *Bcl-2*, and *caspase-3* proteins in each group of cells. In the RG, *Bax* and *caspase-3* levels were added, while *Bcl-2* levels were declined. The changes were more pronounced in the NG, suggesting that Nodakenin can enhance radiotherapy-induced apoptosis.

Table 2. Stati  
and mAs value

**Table 6.** Western blot analysis of the apoptosis-related proteins Bax, Bcl-2, and caspase-3 in A549 cells from each group. CG: control group; RG: radiation group; NG: irradiation + Nodakenin group; Bax: Bcl-2-associated X protein; Bcl-2: B-cell lymphoma-2.

Group	Bax	Bcl-2	caspase-3
CG	1.04±0.01	1.95±0.20	1.03±0.02
RG	1.56±0.12	1.57±0.14	1.49±0.11
NG	2.05±0.20	1.16±0.05	1.95±0.19
Variance ratio	13.209	10.527	15.334
P-value	0.015	0.003	0.024

## DISCUSSION

Radiation therapy is an integral part of the standard treatment for NSCLC. However, its efficacy is often limited by the inherent or acquired radiation resistance of tumor cells. Extensive research has demonstrated that tumor sensitivity to radiation therapy is closely associated with specific intracellular signaling pathways that regulate processes like cell proliferation, DNA damage repair, and apoptosis (15, 16). The AURKA-CXCL5 is closely linked with enhanced invasiveness and increased resistance to chemoradiotherapy in NSCLC cells (17-19). However, the mechanism by which Nodakenin enhances NSCLC radiosensitivity by suppressing the AURKA-CXCL5 axis is still unclear. Research has found that Nodakenin treatment can significantly enhance the response of A549 cells to radiotherapy, as manifested by decreased cell viability and clonogenicity, increased apoptosis, and enhanced  $\gamma$ -H2AX expression. These results suggest that Nodakenin can synergistically induce DNA damage with ionizing radiation and inhibit its repair capacity, thereby enhancing the sensitivity of cells to radiation. This observation is fitted with the conclusion drawn by Choi *et al.* (20). The anti-inflammatory and antioxidant properties of Nodakenin may contribute to alleviating chronic inflammation and oxidative stress in the tumor micro-environment, thereby suppressing tumor growth and metastasis.

Flow cytometry results further confirmed that Nodakenin significantly enhanced radiotherapy-induced apoptosis, supporting its potential role as a radiotherapy sensitizer.  $\gamma$ -H2AX immunofluorescence results showed that DNA damage fluorescence spots increased in the combination therapy group, demonstrating that Nodakenin may exacerbate radiation-induced DNA damage by inhibiting DNA repair mechanisms. Bagnyukova *et al.* and Yu *et al.* have also suggested that Nodakenin can serve as a direct enhancer of cell death, promoting long-term radiosensitivity in cancer cells (21, 22).

Molecular-level analysis indicates that Nodakenin downregulates AURKA and CXCL5 at the mRNA and protein levels and inhibits the activation of the JAK2/STAT3 pathway. This pathway is widely involved in tumor cell drug resistance and immune evasion, and

its inhibition has been shown to enhance the radiotherapy efficacy of various tumor models (23). This is consistent with the observation in this study that Nodakenin enhances radiosensitivity by simultaneously inhibiting multiple pro-survival signals.

Clonogenic assay results demonstrated that Nodakenin treatment weakened the clonogenic growth capacity of NSCLC cells. This suggests that it not only reduces the number of surviving cells but may also affect their long-term proliferative potential. The MAPK and PI3K/Akt signaling pathways, as downstream of AURKA, are also believed to be involved in regulating tumor growth and migration behavior (24, 25). Patel *et al.* reported that inhibiting key factors in the MAPK and PI3K/Akt pathways significantly reduces tumor cell survival and migration capacity, consistent with the findings of this study (26).

Tumor cells often evade radiation-induced cell death by up-regulating anti-apoptotic proteins like Bcl-2 (27, 28). Additionally, Nodakenin may further enhance the cytotoxic effects of radiotherapy by inhibiting cell progression and promoting DNA damage accumulation (29). The upregulation of pro-apoptotic proteins and downregulation of the anti-apoptotic protein Bcl-2 in the Nodakenin treatment group indicate a shift in the apoptotic threshold, which may be associated with mitochondrial dysfunction or endoplasmic reticulum stress. This suggests that Nodakenin may enhance cellular sensitivity to DNA damage and metabolic stress by activating endogenous apoptotic signaling pathways.

In summary, this research exhibits that Nodakenin improves the radiosensitivity of NSCLC cells by simultaneously inhibiting the AURKA-CXCL5 axis and the JAK2/STAT3 signaling pathway. These findings exhibit a theoretical basis for Nodakenin as an adjuvant therapy in NSCLC radiotherapy.

However, the study is subject to certain limitations. First, the experiment was only conducted on a single NSCLC A549 cell line, and the generalizability of the results should be verified in more cell models and in vivo animal experiments. Second, although changes in key signaling protein expression are observed, causal relationships have not been confirmed using siRNA or pathway inhibitors. Future research will aim to validate the radiosensitizing effects of Nodakenin in multiple models and in vivo environments, and clarify its potential mechanisms through molecular targeting methods, thereby providing stronger support for its potential clinical translation. Additionally, considering the multifaceted role of the tumor microenvironment in regulating treatment resistance, the effects of Nodakenin may extend beyond the inhibition of intracellular signaling pathways in tumor cells. The downregulation of CXCL5 expression observed in the study suggests that

Nodakenin may enhance antitumor immune responses under radiotherapy by alleviating immune suppression. Future studies could further explore the drug's impact on immune cell infiltration levels and cytokine profiles in tumor tissues. In clinical applications, Nodakenin, as a radiotherapy sensitizer, holds promise as a low-toxicity adjuvant therapy option for NSCLC patients unsuitable for intensive chemoradiotherapy. Its natural origin and multifaceted effects, including inhibiting tumor cell proliferation, inducing apoptosis, suppressing invasion, and impairing repair, demonstrate promising translational potential, warranting validation through Phase I/II clinical trials. However, systematic pharmacokinetic and toxicity assessments are still required prior to clinical implementation. Future studies will also explore the synergistic effects of Nodakenin in combination with immune checkpoint inhibitors or PARP inhibitors.

**Conflict of interests:** None

**Funding:** Not applicable

**Ethical consideration:** This research was performed in line with the principles of the Declaration of Helsinki, which was approved by the Ethics Committee of Affiliated Hospital of Hebei University.

**Authors' contributions:** X.W.: Conceptualization, formal analysis, methodology, project administration, writing - original draft. R.T.: Conceptualization, investigation, methodology, writing - original draft. K.D.: Data curation, formal analysis, project administration. X.Z.: Data curation, investigation, project administration, supervision, validation, writing - review & editing.

## REFERENCES

- Riely GJ, Wood DE, Ettinger DS, Aisner DL, Akerley W, Bauman JR, et al. (2024) Non-small cell lung cancer, version 4.2024, NCCN clinical practice guidelines in oncology. *J Natl ComprCancNetw*, **22**: 249-274.
- Remon J, Soria JC, Peters S (2021) Early and locally advanced non-small-cell lung cancer: an update of the ESMO Clinical Practice Guidelines focusing on diagnosis, staging, systemic and local therapy. *Ann Oncol*, **32**: 1637-1642.
- Li HL, Wang JX, Dai HW, Liu JJ, Liu ZY, Zou MY, et al. (2023) Prognostic prediction value and biological functions of non-apoptotic regulated cell death genes in lung adenocarcinoma. *Chin Med Sci J*, **38**: 178-190.
- Deng J, Ma X, Ni Y, Li X, Xi W, Tian M, et al. (2022) Identification of CXCL5 expression as a predictive biomarker associated with response and prognosis of immunotherapy in patients with non-small cell lung cancer. *Cancer Med*, **11**: 1787-1795.
- Yin S, Yu Y, Wu N, Zhuo M, Wang Y, Niu Y, et al. (2024) Patient-derived tumor-like cell clusters for personalized chemo- and immunotherapies in non-small cell lung cancer. *Cell Stem Cell*, **31**: 717-733.
- Yang P, He S, Ye L, Weng H (2024) Transcription factor ETV4 activates AURKA to promote PD-L1 expression and mediate immune escape in lung adenocarcinoma. *Int Arch Allergy Imm*, **185** (9): 910-920.
- Lei Q, Zhen S, Zhang L, Zhao Q, Yang L, Zhang Y (2024) A2AR-mediated CXCL5 upregulation on macrophages promotes NSCLC progression via NETosis. *Cancer Immunol Immun*, **73**(6): 108.
- Du R, Huang C, Liu K, Li X, Dong Z (2021) Targeting AURKA in cancer: molecular mechanisms and opportunities for cancer therapy. *Molecular Cancer*, **20**: 1-27.
- Park JG, Jeon H, Shin S, Song C, Lee H, Kim NK, Lee IG (2023) Structural basis for CEP192-mediated regulation of centrosomal AURKA. *Science Advances*, **9**(16): eadf8582.
- Wang Y, Liu J, Xu J, Ji Z (2025) The expression and prognosis for Aurora kinases in human non-small cell lung cancer. *Discover Oncology*, **16**(1): 1-19.
- Shah B and Solanki N (2025) Ameliorative effect of nodakenin in combating TNBS-induced ulcerative colitis by suppressing NFκB-mediated NLRP3 inflammasome pathway. *Naunyn-Schmiedeberg's Archives of Pharmacology*, **398**(1): 673-686.
- Chung KS, Heo SW, Lee JH, Han HS, Kim GH, Kim YR, Lee KT (2025) Protective potential of nodakenin in high-fat diet-mediated colitis-associated cancer: Inhibition of STAT3 activation and Wnt/β-catenin pathway, and gut microbiota modulation. *International Immunopharmacology*, **157**: 114734.
- Wang J, Hu T, Wang Q, Chen R, Xie Y, Chang H, Cheng J (2021) Repression of the AURKA-CXCL5 axis induces autophagic cell death and promotes radiosensitivity in non-small-cell lung cancer. *Cancer Letters*, **509**: 89-104.
- Wang X, Tian R, Duan K, Zhang X (2024) Nodakenin inhibits AURKA-CXCL5 axis induced autophagy and apoptosis in non-small cell lung cancer and promotes radiosensitivity of cancer cells. *Pakistan Journal of Zoology*, **56**: 3463-3467.
- Saini S and Gurung P (2025) A comprehensive review of sensors of radiation-induced damage, radiation-induced proximal events, and cell death. *Immunological reviews*, **329**(1): 13409.
- Shang T, Jia Z, Li J, Cao H, Xu H, Cong L, Liu J (2025) Unraveling the triad of hypoxia, cancer cell stemness, and drug resistance. *Journal of Hematology & Oncology*, **18**(1): 32.
- Jasper K, Stiles B, McDonald F, Palma DA (2022) Practical management of oligometastatic non-small-cell lung cancer. *J Clin Oncol*, **40**: 635-641.
- Ettinger DS, Wood DE, Aisner DL, Akerley W, Bauman JR, Bharat A, et al. (2022) Non-small cell lung cancer, version 3.2022, NCCN clinical practice guidelines in oncology. *J Natl ComprCancNetw*, **20**: 497-530.
- Li Y, Sun C, Tan Y, Zhang H, Li Y, Zou H (2021) ITGB1 enhances the radioresistance of human non-small cell lung cancer cells by modulating the DNA damage response and YAP1-induced epithelial-mesenchymal transition. *Int J Biol Sci*, **17**: 635-650.
- Choi HS, Ku JK, Ko SG, Yun PY (2025). Anticancer effects of SH003 and its active component Cucurbitacin D on oral cancer cell lines via modulation of EMT and cell viability. *Oncol Res*, **33**(5): 1217.
- Bagnyukova T, Egleston BL, Pavlov VA, Serebriiskii IG, Golemis EA, Borghaei H (2024) Synergy of EGFR and AURKA inhibitors in KRAS-mutated non-small cell lung cancers. *Cancer Res Commun*, **4**: 1227-1239.
- Yu H, Liu J, Bu X, Ma Z, Yao Y, Li J, et al. (2024) Targeting METTL3 reprograms the tumor microenvironment to improve cancer immunotherapy. *Cell Chem Biol*, **31**: 776-791.
- Zhou YC, Zhu HL, Pang XZ, He Y, Shen Y, Ma DY (2025) The IL-6/STAT3 signaling pathway is involved in radiotherapy-mediated upregulation of PD-L1 in esophageal cancer. *Ann Clin Lab Sci*, **55** (1): 28-38.
- Grisetti L, Garcia C J, Saponaro A A, Tiribelli C, Pascut D (2024) The role of Aurora kinase A in hepatocellular carcinoma: Unveiling the intriguing functions of a key but still underexplored factor in liver cancer. *Cell Proliferation*, **57**(8): 13641.
- Nasimi Shad A, Akhlaghipour I, Alshakarchi H I, Saburi E, Moghbeli M (2024) Role of microRNA-363 during tumor progression and invasion. *Journal of Physiology and Biochemistry*, **80**(3): 481-499.
- Patel K and Patel DK (2024) Understanding the anti-cancer effects of phytochemicals on prostate cancer: a promising lead for drug discovery in medicine. *EJMA*, **4**(4): 191-197.
- He X, Wei Y, Wu S, Huang F, Zhang K (2024) Diffusion characteristics of diffusion-weighted imaging in children with hippocampus injury during complex acute febrile seizure: a prospective observational study. *Int J Radiat Res*, **22**(4): 971-975.
- Huang S, Xu M, Deng X, Da Q, Li M, Huang H, et al. (2024) Anti irradiation nanoparticles shelter immune organ from radio-damage via preventing the IKK/κB/NF-κB activation. *Mol Cancer*, **23**(1): 234.
- Ershov P, Poyarkov S, Konstantinova Y, Veselovsky E, Makarova A (2023) Transcriptomic signatures in colorectal cancer progression. *Curr Mol Med*, **23**: 239-249.